Computers and Mathematics with Applications 65 (2013) 1558–1574

Contents lists available at SciVerse ScienceDirect

Computers and Mathematics with Applications

journal homepage: www.elsevier.com/locate/camwa

# A hierarchy of maximum entropy closures for Galerkin systems of incompressible flows

Bernd R. Noack [a,*], Robert K. Niven [b]

[a] Institute PPRIME, CNRS – Université de Poitiers – ENSMA, UPR 3346, Département Fluides, Thermique, Combustion, CEAT, 43 rue de l'Aérodrome, F-86036 POITIERS Cedex, France

[b] School of Engineering and Information Technology, The University of New South Wales, Australian Defense Force Academy, Northcott Drive, Canberra Act 2600, Australia

ARTICLE INFO

*Keywords:*
Nonlinear dynamic system
Ergodic measure
Jaynes maximum entropy principle

ABSTRACT

We propose a maximum-entropy closure strategy for dissipative dynamical systems building on and generalizing earlier examples (Noack & Niven (2012) [11]). Focus is placed on Galerkin systems arising from a projection of the incompressible Navier–Stokes equation onto orthonormal expansion modes. The maximum-entropy closure is motivated by a simple analytical example and elaborated to a hierarchical framework with sufficient conditions for the existence of solutions.



## 1. Introduction

We generalize a maximum-entropy closure for the ergodic measure of a class of dissipative dynamical systems arising from fluid mechanics. The derivation of statistical properties of dynamical systems falls in the realm of ergodic theory. Also the turbulence closure problem, which R. Feynman highlights as '*the most important unsolved problem of classical physics*', falls in this category.

A beautiful closure of a dynamical system has been proposed by Maxwell and Boltzmann over 150 years ago [1]. They derived the Gaussian probability density function (PDF) of the velocities of the molecules of an ideal gas. This implies that the Newtonian laws with elastic collisions of myriad of molecules do not need to be integrated if one is just interested in the velocity probability distribution. In hindsight, this result is not surprising. The evolution equation has many symmetries. For instance, there is no reason why one molecule should have a different PDF from another one. In addition, all space directions are indistinguishable as well. Finally, the Gaussian PDF arises naturally from the law of large numbers, i.e. by averaging over myriad of flights between two collisions.

Over 50 years ago, Jaynes [2,3] laid the foundation for an elegant information theoretic derivation for a gas with hard elastic collisions. This closure is remaining the source of inspiration for statistical turbulence theory. W. Heisenberg optimistically wrote [4]:

> *Turbulence is an essentially statistical problem of the same type as one meets in statistical mechanics, since it is the problem of distribution of energy among a very large number of degrees of freedom. Just as in Maxwell–Boltzmann theory this problem can be solved without going into any details of the mechanical motion, so it can be solved here by simple considerations of similarity.*

* Corresponding author. Tel.: +33 549 366015; fax: +33 549 366015.
*E-mail addresses:* Bernd.Noack@univ-poitiers.fr (B.R. Noack), R.Niven@adfa.edu.au (R.K. Niven).
*URL:* http://BerndNoack.com (B.R. Noack).

0898-1221/$ – see front matter 
http://dx.doi.org/10.1016/j.camwa.2013.02.016

Since then, there exist numerous entropic investigations of the Navier–Stokes equation or idealizations thereof [5–8]. Yet, none arrives at the Kolmogorov cascade without invoking similar assumptions.

Entropic closures appear more promising for reduced-order Galerkin models describing coherent structure dynamics of incompressible flows [9,10]. The authors have recently presented a successful closure for a wake model [11]. In the current study, this path is pursued and extended by a simple analytical closure example and a general closure strategy for more complex systems. The focus is placed on a dynamical system closure—not on the associated fluid mechanics aspects.

The manuscript is organized as follows. In Section 2, the MaxEnt closure is exemplified and elaborated for the three-dimensional mean-field model. In Section 3, a closure strategy is proposed for general class of Galerkin systems. In Section 4, the closure strategy is applied to Galerkin models of the cylinder wake and mixing layer. Finally (Section 5), the main results are summarized.

## 2. MaxEnt closure for a mean-field model—an introductory example

In this section, we elaborate a maximum entropy (MaxEnt) closure for a simple Galerkin system: a mean-field model which describes a large class of oscillatory flows. This introductory example provides analytical insights and motivates a more general MaxEnt closure in the following sections. First (Section 2.1), the underlying assumptions for the Galerkin system are explained. This leads to the formulation of the MaxEnt closure concept in Section 2.2. Then (Section 2.3), the mean-field system is recapitulated as a first application. In Section 2.4, the first MaxEnt closure is presented. A more accurate closure incorporates stability properties of the mean flow (Section 2.5). Finally (Section 2.6), alternative constraints are discussed.

### 2.1. Dynamical properties of Galerkin systems

The goal of our study is an entropic closure formalism for low-order statistical moments of incompressible flows. The entropy definition for the infinite-dimensional space of such Navier–Stokes solutions poses serious technical challenges. Hence, we restrict ourselves to flows which can be arbitrarily accurately approximated by a finite-dimensional Galerkin model. In particular, we assume a stationary domain $\Omega$, time-independent boundary conditions, and that the flow state is embedded in the Hilbert space of square-integrable vector fields $\mathcal{L}_2(\Omega)$. The corresponding inner product of $\boldsymbol{v}, \boldsymbol{w} \in \mathcal{L}_2(\Omega)$ is defined by

$$(\boldsymbol{v}, \boldsymbol{w})_\Omega := \int_\Omega d\boldsymbol{x}\, \boldsymbol{v} \cdot \boldsymbol{w}, \tag{1}$$

and the associated norm reads $\|\boldsymbol{v}\|_\Omega := \sqrt{(\boldsymbol{v}, \boldsymbol{v})_\Omega}$. The sign ':=' implies that the left-hand side is defined by the right-hand side.

The resulting Galerkin models are based on a steady base flow $\boldsymbol{u}_0$ and a modal expansion for the fluctuation with $N$ modes $\boldsymbol{u}_i,\ i = 1, \ldots, N$, and the corresponding mode amplitudes $a_i$:

$$\boldsymbol{u}(\boldsymbol{x}, t) = \boldsymbol{u}_0(\boldsymbol{x}) + \sum_{i=1}^{N} a_i(t)\, \boldsymbol{u}_i(\boldsymbol{x}). \tag{2}$$

The base flow may be the steady or averaged Navier–Stokes solution. The expansion modes may be a subset of a complete Hilbert-space basis or physical eigenmodes of a linear Navier–Stokes-related equation or arise from empirical data compression. The reader is referred to [12,13,9,10] for detailed mathematical, numerical and physical discussions of the Galerkin method. Without loss of generality, we assume that the modes $\boldsymbol{u}_i$ are orthonormal, i.e.

$$\left(\boldsymbol{u}_i, \boldsymbol{u}_j\right)_\Omega = \delta_{ij}, \quad i, j = 1, \ldots, N. \tag{3}$$

Now, the flow state is approximated by an $N$-dimensional vector $\boldsymbol{a} = [a_1, \ldots, a_N]^\dagger \in \mathcal{R}^N$. The dagger subscript '†' denotes the transpose. Its temporal evolution is described by the propagator $\boldsymbol{a} \mapsto \boldsymbol{f} = [f_1, \ldots, f_N]^\dagger \in \mathcal{R}^N$ via the autonomous dynamical system of ordinary equations, defined as *Galerkin system*,

$$\frac{d\boldsymbol{a}}{dt} = \boldsymbol{f}(\boldsymbol{a}). \tag{4}$$

The solutions are described by a flow map $\boldsymbol{a}(t + \tau) = \boldsymbol{\Phi}_\tau\, (\boldsymbol{a}(t))$ for any $\tau \geq 0$.

This Galerkin system has additional simplifying properties which will be exploited in the MaxEnt closure [11]. First, the Galerkin projection onto the Navier–Stokes equations leads to a propagator with constant, linear and quadratic terms:

$$f_i = c_i + \sum_{j=1}^{N} c_{ij}\, a_j + \sum_{j,k=1}^{N} c_{ijk}\, a_j\, a_k, \quad i = 1, \ldots, N. \tag{5}$$

Secondly, the quadratic is energy preserving for orthonormal bases (3) and for the most common boundary conditions:

$$c_{ijk} + c_{ikj} + c_{jik} + c_{jki} + c_{kij} + c_{kji} = 0, \quad i, j, k = 1, \ldots, N. \tag{6}$$

Thirdly, any realistic Galerkin system is dissipative and has constant negative divergence

$$\nabla_{\boldsymbol{a}} \boldsymbol{f} := \sum_{i=1}^{N} \frac{\partial f_i}{\partial a_i} = \sum_{i=1}^{N} c_{ii} < 0. \tag{7}$$

The lack of quadratic coefficients is a consequence of the energy preservation (6). Physically, (7) implies that the Galerkin system has enough stable dissipative directions which can absorb the energy produced by the large scales. Dynamically, (7) implies that the phase volume shrinks exponentially fast and that bounded trajectories converge to one attractor.

And fourthly, most Galerkin systems have a single axiom A attractor [14]. These systems have a single connected bounded set of point $\mathcal{A} \subset \mathcal{R}^N$ to which almost all solutions of (4) – possibly only in a neighbourhood of $\mathcal{A}$ – converge. This further implies that the temporal average of any real or tensor-valued state function $\boldsymbol{F}(\boldsymbol{a})$,

$$\overline{\boldsymbol{F}(\boldsymbol{a})} := \lim_{T\to\infty} \frac{1}{T} \int_0^T dt\, \boldsymbol{F}\left(\boldsymbol{a}(t)\right), \tag{8}$$

is independent of the initial condition $\boldsymbol{a}(0)$. This independence is the working assumption of statistical fluid mechanics (see, e.g. [15,16]).

Moreover, the long-term behaviour of (4) is characterized by an ergodic measure $p_{\mathcal{A}}(\boldsymbol{a})$. This measure is a probability density function (PDF) of $\boldsymbol{a}$: $p_{\mathcal{A}}(\boldsymbol{a})\, d\boldsymbol{a}$, $d\boldsymbol{a} = da_1\, da_2 \cdots da_N$ is the probability that the state is in the parallelepiped $[a_1, a_1 + da_1] \times [a_2, a_2 + da_2] \times \cdots \times [a_N, a_N + da_N]$. The probability to find the state anywhere in space is unity,

$$\int_{\mathcal{R}^N} d\boldsymbol{a}\, p_{\mathcal{A}}(\boldsymbol{a}) = 1. \tag{9}$$

The measure defines an ergodic average – also called ensemble average – of any state function,

$$\langle \boldsymbol{F}(\boldsymbol{a}) \rangle_{p_{\mathcal{A}}} := \int_{R^N} d\boldsymbol{a}\, p_{\mathcal{A}}(\boldsymbol{a})\, \boldsymbol{F}(\boldsymbol{a}). \tag{10}$$

For a dynamical system with an axiom A attractor, the ergodicity property holds, i.e. time and ergodic averages are equal,

$$\langle \boldsymbol{F}(\boldsymbol{a}) \rangle_{p_{\mathcal{A}}} = \overline{\boldsymbol{F}(\boldsymbol{a})}. \tag{11}$$

### 2.2. Maximum entropy principle for Galerkin systems

The existence of an ergodic measure $p_{\mathcal{A}}(\boldsymbol{a})$ inspires the search for an entropic approximation $p(\boldsymbol{a})$. Following Jaynes [3], let $q(\boldsymbol{a})$ be our prior PDF. This PDF can be seen as our first choice before any additional knowledge of the constraints. The improper prior $q \equiv 1$ is a common choice since it gives no a prior preference to any state space element. The lack of normalisability does not affect the result as can be shown by a limiting consideration.

The prior will generally not be compatible with additional knowledge, e.g. with constraints of the form

$$\langle G_k(\boldsymbol{a}) \rangle = g_k, \quad k = 1, \ldots, K, \tag{12}$$

where $G_k$ are state functions of $\boldsymbol{a}$ and $g_k$ are constant values. Here, and in the following, the angular brackets shall indicate the ergodic average with respect to the PDF we consider.

Now, we try to be as close to the prior as possible respecting the constraints. Or, equivalently, we try to preserve the largest set of possibilities. Following the conventional methodology (see, e.g. [17,18,3]), this leads to the maximization of the Kullback–Leibler entropy defined by

$$H := -\int_{\mathcal{R}^N} d\boldsymbol{a}\, p(\boldsymbol{a})\, \ln\left[\frac{p(\boldsymbol{a})}{q(\boldsymbol{a})}\right] = -\left\langle \ln\left[\frac{p(\boldsymbol{a})}{q(\boldsymbol{a})}\right]\right\rangle. \tag{13}$$

Here, the joint prior probability density function $q$ is also required for reasons of dimensional consistency, since the logarithm of a dimension has no meaning. Even more importantly, the prior is required to ensure that $H$ possesses the property of scale invariance [19, pp. 72–78].

Summarizing, the MaxEnt closure of the Galerkin system (4) is given by the MaxEnt principle (14), the normalization condition (9), and the additional constraints (12).

$$H = -\left\langle \ln\left[\frac{p(\boldsymbol{a})}{q(\boldsymbol{a})}\right]\right\rangle = \max \tag{14a}$$

$$\text{subject to} \quad \langle 1 \rangle = 1 \tag{14b}$$

$$\text{and} \quad \langle G_k(\boldsymbol{a}) \rangle = g_k, \quad m = 1, \ldots, K. \tag{14c}$$

A key enabler for accurate predictions are suitable constraints (14c). In the following, the mean-field system is considered and a corresponding MaxEnt closure derived.

### 2.3. Mean-field Galerkin system

A least-order Galerkin model ($N = 3$) is considered describing transients from an unstable steady solution to stable periodic oscillations for a large class of oscillatory fluid flows. $a_1$ and $a_2$ define amplitude and phase of an oscillatory fluctuation, $a_3$ parametrizes the base-flow evolution. For details, the reader is referred to the original publications of Stuart and Watson summarized in [20] and generalizations of the authors [21,22]. In this study, the numerical values of the minimal POD Galerkin model [21] for the cylinder wake shedding are taken.

Under mean-field assumptions, the Galerkin system (4) simplifies to

$$da_1/dt = (\sigma_1 - \beta\, a_3)\; a_1 - (\omega_1 + \gamma\, a_3)\; a_2, \tag{15a}$$

$$da_2/dt = (\sigma_1 - \beta\, a_3)\; a_2 + (\omega_1 + \gamma\, a_3)\; a_1, \tag{15b}$$

$$da_3/dt = \sigma_0\, a_3 + \alpha\, \left(a_1^2 + a_2^2\right). \tag{15c}$$

Here, the numerical Galerkin system parameters satisfy $\sigma_1 > 0, \beta > 0, \sigma_0 < 0$ as necessary prerequisites for a globally stable periodic solution. Without loss of generality, $\omega_1 > 0$ for reasons of convenience. Moreover, $\gamma > 0$ by numerical observation.

The mean-field system (15) has one unstable fixed point $a_1 = a_2 = a_3 = 0$ representing the unstable steady Navier–Stokes solution and a periodic solution representing vortex shedding. The periodic solution reads (modulo a phase shift):

$$a_1 = R\, \cos \Omega t, \qquad a_2 = R\, \sin \Omega t, \qquad a_3 = B, \tag{16}$$

where

$$B = \frac{\sigma_1}{\beta}, \qquad R = \sqrt{-\frac{\sigma_0\, \sigma_1}{\alpha\, \beta}}, \qquad \Omega = \omega_1 + \frac{\sigma_1\, \gamma}{\beta}.$$

The negative sign under the square-root guarantees a real amplitude, since $\sigma_1, \alpha, \beta > 0$ and $\sigma_0 < 0$.

The mean-field system encapsulates the mean-field variation as the only amplitude-limiting mechanism. The growth-rate of the oscillatory fluctuation with amplitude $r_1 := \sqrt{a_1^2 + a_2^2}$ is given by

$$\widetilde{\sigma}_1 := \frac{1}{r_1}\, \frac{dr_1}{dt} = \sigma_1 - \beta\, a_3. \tag{17}$$

If the fluctuation energy is too large $r_1 > R$, the shift-mode amplitude eventually exceeds the asymptotic value $a_3 > B$, and a negative growth-rate $\widetilde{\sigma}_1 < 0$ dampens the fluctuation. In the case $r_1 < R$, the opposite mechanism increases the fluctuation energy. In other words, low frequencies stabilize the harmonic fluctuations.

The coefficients $\sigma_1$ and $\omega_1$ of the linear term are taken from the Galerkin projection. $\sigma_0$ is calibrated from a DNS simulation transient [23]. The coefficients of the nonlinear terms $\alpha$, $\beta$ and $\gamma$ need to account for the neglected higher harmonics. We calibrate them against the DNS solution:

$$R = R^\bullet = \sqrt{\overline{(a_1^\bullet)^2} + \overline{(a_2^\bullet)^2}}, \qquad B = B^\bullet = \overline{a_3^\bullet}, \qquad \Omega = \Omega^\bullet. \tag{18}$$

The full circle superscript '$\bullet$' indicates a value of the DNS simulation.

### 2.4. MaxEnt closure with the improper prior

The starting point is the three-dimensional autonomous system (15). In the first step, we exploit that the solution quickly approaches the mean-field manifold and the shift mode amplitude $a_3$ can be slaved to $a_1$ and $a_2$ [21]. Then, $da_3/dt \equiv 0$ and (15c) yields the paraboloidal manifold

$$a_3 = \alpha^m \left(a_1^2 + a_2^2\right), \quad \alpha^m = -\alpha/\sigma_0. \tag{19}$$

The superscript '$m$' denotes quantities associated with the mean-field manifold. Substituting (19) in (15a) and (15b) yields

$$da_1/dt = \left[\sigma_1 - \beta^m \left(a_1^2 + a_2^2\right)\right]\; a_1 - \left[\omega_1 + \gamma^m \left(a_1^2 + a_2^2\right)\right]\; a_2 \tag{20a}$$

$$da_2/dt = \left[\sigma_1 - \beta^m \left(a_1^2 + a_2^2\right)\right]\; a_2 + \left[\omega_1 + \gamma^m \left(a_1^2 + a_2^2\right)\right]\; a_1 \tag{20b}$$

where $\beta^m = \beta\, \alpha^m = -\alpha\, \beta/\sigma_0$ and $\gamma^m = \gamma\, \alpha^m = -\alpha\, \gamma/\sigma_0$. In polar coordinates $(r_1, \theta_1)$ with $a_1 + \imath a_2 = r_1\, e^{\imath\theta_1}$ ('$\imath$': imaginary unit), (20) becomes the Landau equation for a supercritical Hopf bifurcation,

$$dr_1/dt = \sigma_1 r_1 - \beta^m r_1^3, \tag{21a}$$

$$d\theta_1/dt = \omega_1 + \gamma^m r_1^2. \tag{21b}$$

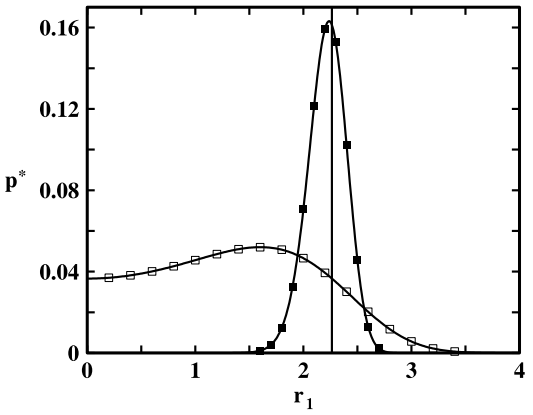


**Fig. 1.** Probability distribution $p^*(r_1)$ for the mean-field model (15). The curves marked with the symbols (□) and (■) represent the MaxEnt predictions with improper prior (26) and marginal stability prior (30), respectively. The latter results are explained in the following section. The vertical line $r_1 = R^\bullet = 2.2646$ marks the DNS value.

The form of the Landau equation immediately reveals the phase invariance of (20). Already by symmetry, the centre of the limit-cycle attractor coincides with the origin.

The MaxEnt closure (14) shall be applied to the two-dimensional Landau system (20). The closure is based on improper prior $q \equiv 1$, on the PDF $p = p(a_1, a_2)$ with $N = 2$, on the Kullback–Leibler entropy (13), and on the normalization constraint (9). The non-Hamiltonian nature of the underlying evolution equation prohibits a fixed unknown energy as constraint [24, Section 4.11]. However, on average the total power must vanish, i.e. there cannot be an average net production of fluctuation energy $K = \langle a_1^2 + a_2^2 \rangle / 2$. The (averaged) total power is defined by

$$P := \left\langle \frac{dK}{dt} \right\rangle = \left\langle a_1 \frac{da_1}{dt} + a_2 \frac{da_2}{dt} \right\rangle. \tag{22}$$

From (20) and (22), a vanishing total power implies

$$P = \sigma_1 \langle r_1^2 \rangle - \beta^m \langle r_1^4 \rangle = 0. \tag{23}$$

Summarizing, the resulting MaxEnt problem reads

$$H = -\left\langle \ln \left[ \frac{p(a_1, a_2)}{q(a_1, a_2)} \right] \right\rangle \stackrel{!}{=} \max, \quad q \equiv 1 \tag{24a}$$

$$\text{subject to} \quad \langle 1 \rangle = 1 \tag{24b}$$

$$\text{and} \quad \sigma_1 \langle r_1^2 \rangle - \beta^m \langle r_1^4 \rangle = 0. \tag{24c}$$

In the following, the MaxEnt problem (24) is solved. A straight-forward Lagrange formalism (see, e.g., [11]) yields the PDF

$$p^* = \exp\left[1 - \lambda_0 - \zeta \left(\sigma_1 r_1^2 - \beta^m r_1^4\right)\right] \tag{25}$$

where the superscript '$*$' denotes the solution, $\lambda_0$ the Lagrange multiplier corresponding to normalization (24b) and $\zeta$ is the Lagrangian multiplier conjugate to the total power balance constraint (24c). Normalization (24b) gives

$$\begin{aligned} p^* &= \frac{1}{Z_A} \exp\left[-\zeta \left(\sigma_1 r_1^2 - \beta^m r_1^4\right)\right], \\ Z_A &= 2\pi \int_0^\infty dr_1 \, r_1 \exp\left[-\zeta \left(\sigma_1 r_1^2 - \beta^m r_1^4\right)\right], \end{aligned} \tag{26}$$

where $Z_A$ is the partition function.

The PDF has a maximum at $r_1 = \sqrt{2}R/2$, i.e. not too far from the DNS radius. The remaining tasks are the determination of the partition function $Z_A$ and the Lagrangian multiplier $\zeta$.

The total power (23) converges to $-\infty$ as $\zeta \to 0^+$, is monotonically increasing for $\zeta > 0$ until a maximum at $\zeta_{\max}$ and converges to 0 as $\zeta \to \infty$. Most importantly, it has a single zero $\zeta^* = k/R^2 \approx 5.56 \in (0, \zeta_{\max})$ signifying the solution to the MaxEnt problem. The parameter $k$ is determined numerically with a Newton iteration. The partition function is computed from (26). We shall not pause to explicate the long and not very illuminating computations.

The resulting predicted PDF (26) is depicted in Fig. 1 (curve marked by '□'). This PDF has a local non-vanishing minimum near the fixed point. The expectation value of the radius $\langle r_1 \rangle$ is about 13% too low. The fluctuation energy $E = \langle r_1^2 \rangle / 2$ is 24% too low.

The MaxEnt closure does not include stability properties of the dynamical system. The unstable fixed point at $r_1 = 0$ has an unphysical finite population probability. Hence, better prediction can be expected if the MaxEnt principle 'is taught' the relation between unstable fixed points and vanishing population. The following section addresses this scope for improvement.

### 2.5. MaxEnt closure with a marginal stability prior

The unstable fixed point at $r_1 = 0$ has a positive growth-rate $\sigma_1 > 0$. In contrast, the centre of the limit cycle of (15) has vanishing growth-rate $\widetilde{\sigma}_1 = \sigma_1 - \beta\, B = 0$. In fact, marginal stability has been postulated for all mean flows [25] and is frequently numerically observed. One example is the considered cylinder wake [26].

We wish to avoid the population of strongly unstable or strongly stable regions, taking the maximum growth rate $\sigma_1$ as our reference scale. This condition may be entered in MaxEnt by introducing a weak prior towards marginal stability:

$$\widetilde{\sigma}_1 = \sigma_1 - \beta\, a_3 = \sigma_1 - \beta^m\, r_1^2 \;\in\; N(0, \sigma_1). \tag{27}$$

Here, $N(0, \sigma_1)$ represents a Gaussian distribution with vanishing mean and standard deviation $\sigma_1$. This yields:

$$\begin{aligned} q &= \frac{1}{Z_q}\, \exp\left[-\frac{\left(r_1^2 - R^2\right)^2}{2R^4}\right], \\ Z_q &= 2\,\pi \int_0^\infty dr_1\, r_1\, \exp\left[-\frac{\left(r_1^2 - R^2\right)^2}{2R^4}\right] = \frac{\pi^{3/2} R^2}{\sqrt{2}}\left(1 + \operatorname{erf}\left[\frac{1}{\sqrt{2}}\right]\right), \end{aligned} \tag{28}$$

where the partition function $Z_q$ is obtained from the standard normalization procedure

$$\int_{-\infty}^{\infty} da_1 \int_{-\infty}^{\infty} da_2\, q = 1.$$

Note that $q(r_1 = 0)/q(r_1 = R) = 1/\sqrt{e}$, i.e. the prior probability density at the fixed point is only about 39% smaller than at the limit cycle.

The resulting MaxEnt problem consists of (24) replacing the improper prior $q \equiv 1$ with a weak prior towards marginal stability (28). The resulting PDF reads

$$\begin{aligned} p^* &= \frac{1}{Z_B}\, q\, \exp\left[-\zeta\left(\sigma_1 r_1^2 - \beta^m r_1^4\right)\right], \\ Z_B &= 2\pi \int_0^\infty dr_1\, r_1\, q\, \exp\left[-\zeta\left(\sigma_1 r_1^2 - \beta^m r_1^4\right)\right], \end{aligned} \tag{29}$$

with the partition function $Z_B$. The only difference between (29) and (26) is the prior $q$. Employing (28), the PDF (29) becomes

$$\begin{aligned} p^* &= \frac{1}{\sqrt{e}\, Z_q\, Z_B}\, \exp\left[-d_1\, r_1^2 - d_2\, r_1^4\right], \\ d_1 &= -\frac{1}{R^2} + \zeta\, \sigma_1, \qquad d_2 = \frac{1}{2R^4} - \zeta\, \beta^m, \end{aligned} \tag{30}$$

or, equivalently,

$$p^* = \frac{1}{Z_q\, Z_B}\, \exp\left[-\frac{\left(R^2 - r_1^2\right)\left(R^2 - r_1^2 + 2\,\zeta\, r_1^2\, R^4\, \beta^m\right)}{2R^4}\right]. \tag{31}$$

The Lagrangian multiplier $\zeta = 87.47$ is determined numerically from the power balance (24c).

The corresponding PDF is displayed in Fig. 1 (see curve marked with '■'). The PDF displays a pronounced peak near the true radius and vanishes near the fixed point. The expectation value $\langle r_1 \rangle$ deviates less than 1% from the DNS value. The total fluctuation energy has an error of only 2%. The inclusion of the weak prior in (30) alone does not explain the dramatic increase in accuracy. In fact, inclusion of the prior increases the numerical value of the Lagrangian multiplier $\zeta$ from 5.56 for the improper prior to 87.47. This increase in $\zeta$ explains the much sharper peak of the PDF.

The prior is parametrized by $q(0)/q(R) = 1/\sqrt{e}$. Decreasing the ratio does not significantly change the PDF. As this ratio converges towards unity, (26) is obtained. The fact that a prior with weak preference of a state space region can give rise to significantly improved accuracy, is a common observation for MaxEnt problems [18,3].

### 2.6. Discussion

The previous MaxEnt closures motivate a general strategy outlined in the following Section 3. As first step, the shift mode has been slaved to the fluctuation level. The shift mode belongs to a general class of A-modes describing low-frequency base-

flow deformations [27,11]. In general, A-modes can be considered functions of the coherent structure fluctuation, resolved by so-called B-modes (see the same sources). Already the first pioneering POD Galerkin model of wall turbulence [28] exploits this slaving relation. In the second step, the dynamics of the B-modes is incorporated in the MaxEnt closure via their total power balance. As final polish, stability properties are incorporated via a weak marginal stability prior. This significantly enhances the accuracy of the closure and reduces the population of the unstable fixed point effectively to zero. The MaxEnt closure of the mean-field model can easily be generalized to the larger class of Galerkin systems, if each mode can be classified as A- or B-mode.

It may be noted that the MaxEnt closure is blind to stability properties of the Galerkin system, like the Hopf-formalism [29], the Millionshtchikov closure [30] and other statistical closure theories. The substitution of $t$ by $-t$ in (15), i.e. the inversion of the stability properties of the fixed point and the limit cycle, does not change the PDF of the MaxEnt closure. The MaxEnt closure favours the invariant periodic Galerkin solution because of its largest extent, independently of its stability properties. This property is fortunate for strange attractors. The accountably many unstable limit cycles are dense in the attractor [14] but have smaller extent. In other words, the MaxEnt closure favours the attractor as opposed to unphysical unstable invariant solutions.

## 3. MaxEnt closure strategy for Galerkin systems

In this section, we develop the building blocks of a MaxEnt closure for general Galerkin systems. In this framework, the mean-field model closure appears as particular example. First (Section 3.1), the ergodicity assumption for the Galerkin system is discussed. Second (Section 3.2), the choice of the entropy is motivated. Then, (Sections 3.3 and 3.4), constraints for the mean flow and for the fluctuations are considered. Higher-order constraints are proposed in the following section (Section 3.5). Finally (Section 3.6), a closure strategy is presented employing simple to refined sets of constraints and a guaranteed existence of solution.

### 3.1. Ergodicity assumption of the Galerkin system

In the entropic closure, we consider dissipative dynamical systems with a single globally stable attractor [14] as mentioned in Section 2.1. The corresponding attractor may result (1) from (trivial) fixed point dynamics, (2) from oscillatory dynamics leading to a limit cycle, (3) from multi-frequency dynamics converging to a torus, or (4) from chaotic/turbulent dynamics leading to a strange attractor with at least one positive Lyapunov exponent. Evidently, a closure is only needed for unsteady dynamics. The assumed single attractor implies ergodicity, i.e. any time-averaged function of the state $\boldsymbol{F}(\boldsymbol{a})$ is equal to the ensemble average. This ergodicity property is fulfilled by most flow configurations, particularly by shear flows.

Ergodicity excludes the existence of multiple attractors, i.e. several different flow states. In this case, the selected attractor of a trajectory depends on the initial condition. Hysteresis with two stable states is a prominent example. The literature contains examples for such configurations, e.g. the drag crisis of the cylinder wake [31], but they are the exception, not the rule. For completeness, we mention that the ergodicity assumption excludes energy-preserving dynamics, like Hamiltonian dynamics.

A statistical closure provides an estimate of the ergodic measure $p(\boldsymbol{a})$. This measure satisfies the steady Liouville equation

$$\nabla_{\boldsymbol{a}} \cdot \boldsymbol{f}(\boldsymbol{a}) = 0. \tag{32}$$

This equation represents a partial differential equation with $N$ independent variables $a_1, \ldots, a_N$. For $N \gg 3$, its numerical solution is an extreme computational challenge, if possible at all.

Intriguingly, Boltzmann derived the Maxwell distribution of molecular velocities of an ideal gas from such a Liouville equation of mechanics exploiting the symmetries of the problem [32]. Unfortunately, symmetries of higher-dimensional Galerkin systems are rare, thus excluding a similar approach. Hence, we follow Jaynes [3] incorporating only select dynamical and statistical properties for reasons of computational costs and analytical insights. It should be noted that the effective support of the analytically approximated ergodic measure can at most be a coarse grained finite-volume coverage of the attractor on a zero set in $\mathcal{R}^N$. For instance, the delta peak of the limit-cycle distribution in Fig. 1 is approximated by a Gaussian bell form.

### 3.2. State space and entropy

Evidently, the MaxEnt closure is affected by the choice of the state space and entropy. We have restricted the discussion to Galerkin models with orthonormal modes spanning the dominant flow structures. Arguably, orthonormal modes are the most natural basis for closures as they harmonize most with key energy considerations: (1) The fluctuation energy can be decomposed in modal contributions; (2) The power balance has also modal counterparts; (3) The quadratic term is energy-preserving. Thus, the mode amplitudes can be considered as generalized velocity components of the fluid flow fluctuation. Non-orthonormal bases, like stability modes of the linearized Navier–Stokes equation, have none of these properties.

Concerning the choice of entropy function, we adopt the Kullback–Leibler or relative entropy form (13). This form arises from the multinomial probability distribution in the asymptotic or continuum limit of an infinite number of particles. This

is consistent with the Boltzmann or combinatorial definition of entropy [32,33] – also adopted in large deviations theory [34,35] – in which we choose the entropy function which, when maximized, yields the most probable state of the system. It is possible that other entropy functions may be more appropriate in some circumstances (such as for flows of bosons or fermions [36]). However, in the absence of evidence to the contrary, there are strong arguments for adoption of the Kullback–Leibler form [3]. This is consistent with the definition used throughout most of statistical physics (see, e.g. [37]).

The improper prior $q \equiv 1$ is chosen as default. If one of the mode amplitudes $a_i$ characterizes a base-flow variation (A-mode), a small preference of marginally stable regions is incorporated in the prior as elaborated in the mean-field example (Section 2.5). This change is justified a priori by the generally observed marginal stability of mean flows and a posteriori by improved predictions. Marginal stability of mean flows has been postulated originally by Malkus [25] and has been employed by him and other authors [38] as rigorous constraint for a variational principle. The marginal stability prior incorporates an important stability property of flows without restraining the state space too much and without causing mathematical complications. Our closure approach is physically well founded: (1) reduction of the dynamics on the inertial manifold derived from the Reynolds equations; (2) constraints for the fluctuations from power considerations; and (3) a weak prior from a stability property. Here, the Reynolds equation is given the highest priority while an empirical observation acts only as weak prior. In principle, other strategies are perceivable, e.g. the inertial manifold may be incorporated as a prior and the marginal stability as a constraint. Arguably such a permutation gives too much weight to an empirical observation and too little weight to a well-justified system reduction.

The employed Reynolds and power balance equations constitute the heart of the closure. They are rigorous deductions from the Galerkin system. The choice of this information from the Galerkin system may even determine the existence of a solution, as the following sections will make clear.

### 3.3. Constraints for the mean flow

First, a closure relation for the centre of the attractor is required. The starting point of this search is the Reynolds decomposition in Galerkin state space (Section 3.3.1). The most general relation is the Galerkin analogue of the Reynolds equation (Section 3.3.2). In some cases, a further simplification can be achieved with the identification of an inertial manifold (Section 3.3.3). Occasionally, symmetries of the Galerkin system can be exploited (Section 3.3.4). For any Galerkin system, we first search for symmetry closures, then for manifolds before the modal Reynolds equations are used.

#### 3.3.1. Reynolds decomposition

The mean-flow closure commences from the Reynolds decomposition of the mode amplitude vector $\boldsymbol{a}$ into a temporal average $\overline{\boldsymbol{a}}$ and a fluctuation $\boldsymbol{a}'$,

$$\boldsymbol{a} = \overline{\boldsymbol{a}} + \boldsymbol{a}'. \tag{33}$$

Throughout this study, ergodicity is assumed, i.e. $\langle F \rangle = \overline{F}$ for any state function $F(\boldsymbol{a})$. The overbar is used when referring to derivations from the Navier–Stokes equation, while the triangular brackets are adopted for moment constraints in the MaxEnt method.

The fluctuation is characterized by the modal energy distribution

$$E_i := \overline{\left(a_i'\right)^2}/2, \quad i = 1, \ldots, N. \tag{34}$$

Owing to the orthonormality of the modes, the modal energy sums up to the total fluctuation energy

$$E := \overline{\|\boldsymbol{u}'\|^2}/2 = \sum_{i=1}^{N} \overline{a_i^2}/2, \tag{35}$$

neglecting the contribution of the expansion residual.

For a POD decomposition of snapshot data, the first moments of the mode amplitudes vanish and the second moments diagonalize,

$$\overline{a_i} = 0, \qquad \overline{a_i\, a_j} = \overline{a_i'\, a_j'} = 2E_i\delta_{ij}. \tag{36}$$

#### 3.3.2. Modal Reynolds equation

The modal analogue of the Reynolds equation can easily be derived from (4) and (33) (see, e.g. [9]):

$$0 = c_i + \sum_{j=1}^{N} c_{ij}\, \overline{a_j} + \sum_{j,k=1}^{N} c_{ijk}\, \overline{a_j}\, \overline{a_k} + \sum_{j,k=1}^{N} c_{ijk}\, \overline{a_j' a_k'}, \quad i = 1, \ldots, N. \tag{37}$$

For POD modes, (36) simplifies (37) to $0 = c_i + 2\sum_{j=1}^{N} c_{ijj}\, E_j$, which can be considered a linear algebraic system for $E_j$, $j = 1, \ldots, N$.

It should be noted that the term $\overline{a_j}\ \overline{a_k}$ of (37) prevents the modal Reynolds equation to be cast in the form (14c). This technical complication can easily be cured by averaging the Galerkin system without employing the Reynolds decomposition. This leads to the equivalent set of equations

$$0 = c_i + \sum_{j=1}^{N} c_{ij}\,\overline{a_j} + \sum_{j,k=1}^{N} c_{ijk}\,\overline{a_j\,a_k}, \quad i = 1, \ldots, N. \tag{38}$$

### 3.3.3. Inertial manifolds

Some modes resolve base-flow variations by design, e.g. the shift mode, some by their symmetry properties, e.g. transverse profiles of a channel flow, and others by their frequency contents, e.g. slowly changing mode amplitudes. These A-modes are strongly damped and have no or very low frequency $\omega \ll \omega_c$, where $\omega_c$ is the characteristic frequency of the dominant fluctuation. Their slow variation is driven by the fluctuation level of the other modes.

To simplify the discussion, let us assume that the $N$th mode has these properties. Let us further assume that the basic mode $\boldsymbol{u}_0$ is the steady solution and, thus, $c_i = 0,\ i = 1, \ldots, N$. In this case, the time derivative of the mode amplitude $a_N$ in (4) can be neglected and $a_N$ is effectively an algebraic function of the remaining modes. This *slaving* approximation can be rigorously derived in several ways. Near Hopf bifurcation, the centre manifold approximation is a method of choice (see, e.g., [39]). For oscillatory flows, Krylov–Bogoliubov or other averaging methods may be applied. Synergetics formulates a rather general slaving principle based on a time-scale argument (see, e.g., [40]). An inertial manifold is one of the most general concepts (see, e.g., [41]). The slaving can be encrypted by $E_N = 0$, interpreting the average as a short-term time average. The manifold may be approximated by

$$a_N = \sum_{j=1}^{N-1} c^m_{Nj}\,a_j + \sum_{j,k=1}^{N-1} c^m_{Njk}\,a_j\,a_k, \tag{39}$$

where the coefficients $c^m_{Nj}$, $c^m_{Njk}$ are derived from (4). Alternatively, the Reynolds equation may be employed for the derivation, like in [28,42,22].

The algebraic equation (39) removes one degree of freedom $a_N$ from the state space. Correspondingly, the ergodic measure is only a function of the first $N-1$ mode amplitudes, $p = p(a_1, a_2, \ldots, a_{N-1})$ and the entropy integral (13) reads

$$H := -\int da_1\,da_2\,\cdots\,a_{N-1}\,p(a_1, a_2, \ldots, a_{N-1})\,\ln\left[\frac{p(a_1, a_2, \ldots, a_{N-1})}{q(a_1, a_2, \ldots, a_{N-1})}\right] \tag{40}$$

modulo an irrelevant constant. The introductory closure example for the mean-field system follows this approach for $N = 3$. The generalization for several algebraic equations is straightforward, e.g. for two shift modes at different frequencies, like in [43].

### 3.3.4. Exploiting symmetries

Let $\boldsymbol{T}\mathring{\boldsymbol{a}} = \boldsymbol{a}$ describe a coordinate transformation from the original state $\boldsymbol{a}$ to the new coordinates $\mathring{\boldsymbol{a}}$ communicated by the non-singular matrix $\boldsymbol{T}$. For oscillatory dynamics, we consider a transformation effecting a rotation in the $a_1, a_2$ plane with angle $\phi$. This transformation is described by

$$\begin{pmatrix}\mathring{a}_1\\ \mathring{a}_2\end{pmatrix} = \begin{pmatrix}\cos\phi & -\sin\phi\\ \sin\phi & \cos\phi\end{pmatrix}\begin{pmatrix}a_1\\ a_2\end{pmatrix} \tag{41}$$

and other coordinates are not affected, $\mathring{a}_i = a_i,\ i = 3, \ldots, N$. If this coordinate transformation does not change the propagator (4), we conclude that the average is invariant under this transformation, i.e.

$$\langle a_1\rangle = \langle a_2\rangle = 0. \tag{42}$$

Similar arguments can be made for many other symmetries. In our examples, only this phase-invariance is invoked. The mean-field model of Section 2 has this property.

## 3.4. Constraints for the fluctuating energy

In this section, two energetic constraints are discussed: the total power balance for the whole Galerkin system (Section 3.4.1) and a refined modal power balance for a single mode (Section 3.4.2).

### 3.4.1. Total power balance

On the attractor, no fluctuation energy $E = \overline{\boldsymbol{a}'\cdot\boldsymbol{a}'}/2$ is created or destroyed on the average. The Galerkin analogue of the turbulent kinetic energy (TKE) power balance is easily be derived by the same technique. The evolution Eq. (4) is multiplied

with $\boldsymbol{a}'$ and averaged (see, e.g. [44,45]). The resulting equation reads:

$$0 = \sum_{i,j=1}^{N} \widetilde{c}_{ij}\, \overline{a_i'\, a_j'} + \sum_{i,j,k=1}^{N} c_{ijk}\, \overline{a_i'\, a_j'\, a_k'}, \tag{43}$$

where $\widetilde{c}_{ij} := c_{ij} + \sum_{k=1}^{N} (c_{ijk} + c_{ikj})\, \overline{a_k}$. The term with quadratic (internal) interactions vanishes for Galerkin systems with energy-preserving quadratic terms. In other words, (6) implies

$$0 = \sum_{i,j=1}^{N} \widetilde{c}_{ij}\, \overline{a_i' a_j'}. \tag{44}$$

For POD modes, (36) implies

$$0 = \sum_{i=1}^{N} \widetilde{c}_{ii}\, E_i. \tag{45}$$

It should be noted that (44) contains product terms like $\overline{a_k}\ \overline{a_i' a_j'}$. Like for the modal Reynolds equation, the Reynolds decomposition prevents an expression of the form (14c). Again, several cures are available. The easiest generally applicable possibility is an analogue derivation for the total energy $E = \overline{\boldsymbol{a}\cdot\boldsymbol{a}}/2$. Now, $E$ quantifies the fluctuation energy around the basic mode $\boldsymbol{u}_0$ which is best taken to be the steady Navier–Stokes solution. In some cases, slaving techniques, like for (23), can be applied. The total power balance may be cast in the form (14c) by introducing $m_i := \overline{a_i}$ as independent variables and re-inserting the Reynolds decomposition $a_i' = a_i - m_i$. In the following, we shall not pause to discuss the curable complications by the Reynolds decomposition.

#### 3.4.2. Modal power balance

Each mode has its own power balance (see, again, [44,45]):

$$0 = \sum_{j=1}^{N} \widetilde{c}_{ij}\, \overline{a_i' a_j'} + \sum_{j,k=1}^{N} c_{ijk}\, \overline{a_i' a_j' a_k'}, \quad i = 1, \ldots, N. \tag{46}$$

The sum of all modal power balances yields the total balance (44).

### 3.5. Higher order constraints

In principle constraints of arbitrary order can be derived. Additional higher-order constraints may be desirable to make the closure more accurate. We discuss two illustrative examples, 4th order constraints derived from the Galerkin system (Section 3.5.1) and 4th order relations from the quasi-normal assumption (Section 3.5.2).

#### 3.5.1. Higher order constraints from the Galerkin system

In principle, many other relationships can be derived for the Galerkin system. Each relationship incorporates additional information from the Galerkin system in the MaxEnt closure. For instance, an equation for the third and fourth centred moments is obtained by averaging the ansatz

$$\frac{d(a_i' a_j' a_k')}{dt} = \frac{da_i'}{dt} a_j' a_k' + a_i' \frac{da_j'}{dt} a_k' + a_i' a_j' \frac{da_k'}{dt} = f_i a_j' a_k' + a_i' f_j' a_k' + a_i' a_j' f_k.$$

The left-hand side vanishes upon averaging while the right-hand side contains moments from 2nd to 4th order. In deriving $O(N^l)$ equations for $l$th order moments, many more unknowns ($O(N^{l+1})$) are created. This leads to the well-known closure problem.

#### 3.5.2. Higher order constraints from the quasi-normal Gaussian approximation

An often-used closure approximation has been proposed by Millionshtchikov [30]. A normal (Gaussian) PDF has vanishing cumulants of third and higher order. The total power balance is not affected by assuming a normal PDF. However, a normal PDF yields vanishing transfer terms in the *modal* power balance (46). Thus, it excludes energy transfer between unstable and dissipative modes. These deficiencies led to the introduction of a more general 'quasi-normal' PDF, with arbitrary third-order moments but vanishing fourth-order cumulants. This leads to the frequently-employed Millionshtchikov closure relation which expresses each centred fourth-order moment by second-order moments:

$$\overline{a_i' a_j' a_k' a_l'} = \overline{a_i' a_j'}\ \overline{a_k' a_l'} + \overline{a_i' a_k'}\ \overline{a_j' a_l'} + \overline{a_i' a_l'}\ \overline{a_j' a_k'}, \quad i, j, k, l = 1, \ldots, N. \tag{47}$$

It should be noted that the Millionshtchikov equation is only an approximation which may or may not be applicable to the considered Galerkin system.

### 3.6. MaxEnt closure strategy

In the previous sections, physical constraints for the MaxEnt problem were derived. Here, combinations of these constraints are discussed. A necessary prerequisite for a successful MaxEnt closure is the existence of its solution. First (Section 3.6.1), a condition for the well-posedness of the MaxEnt problem is outlined. In Section 3.6.2, the classical turbulence closure problem is shown to re-appear in the MaxEnt framework. In the following (Sections 3.6.3–3.6.5), a spectrum from crucial enablers for MaxEnt closures is presented. This spectrum ranges from exploiting dynamic properties to employing empirical information.

For reasons of simplicity, an improper prior $q \equiv 1$ is assumed throughout this section.

#### 3.6.1. Condition for well-posed MaxEnt problem

The MaxEnt closure (14) consists of the maximum entropy principle (14a), the normalization condition (14b) and $K$ side-constraints (14c) describing Galerkin system properties, e.g. (37), (44) or (46). The discussed constraints have the general form $\langle G_k(a_1, \ldots, a_N)\rangle = g_k$, $k = 1, \ldots, K$, where $G_k$ are polynomials in the mode amplitudes and $g_k$ is a real value. The constraints may be cast in vector form $\boldsymbol{G}(\boldsymbol{a}) = \boldsymbol{g}$, where $\boldsymbol{G} := [G_1, \ldots, G_K]^\dagger$ and $\boldsymbol{g} := [g_1, \ldots, g_K]^\dagger$. The solution of the MaxEnt problem (14) has the form

$$p^* = \frac{1}{Z}\, \exp\left[-\boldsymbol{\lambda}\cdot\boldsymbol{G}(\boldsymbol{a})\right], \tag{48}$$

where $\boldsymbol{\lambda} = [\lambda_1, \ldots, \lambda_K]^\dagger$ is a vector comprising the Lagrangian multipliers, $\boldsymbol{\lambda}\cdot\boldsymbol{G}(\boldsymbol{a}) = \sum_{k=1}^{K} \lambda_k G_k(a_1, \ldots, a_N)$, and $Z$ represents the partition function. Integrability of $p^*$ requires that $\boldsymbol{\lambda}\cdot\boldsymbol{G}(\boldsymbol{a})$ increases sufficiently rapidly in all directions, i.e.

$$\boldsymbol{\lambda}\cdot\boldsymbol{G}(\boldsymbol{a}) \to \infty \quad \text{as } \|\boldsymbol{a}\| \to \infty. \tag{49}$$

The existence of a normalizable PDF (48) or, equivalently, (49) is not always guaranteed, as elaborated below.

#### 3.6.2. Closure problem

We consider the discussed constraints derived from the Galerkin system. The modal Reynolds equations (37) leads to $K = N$ constraints with $N(N+1)/2$ independent fluctuation terms $\langle a_i' a_j'\rangle$. The leading order terms of $\boldsymbol{\lambda}\cdot\boldsymbol{G}(\boldsymbol{a})$ in $\boldsymbol{a}'$ are $G_2' := \sum_{i,j,k=1}^{N} \lambda_i\, c_{ijk}\, a_i'\, a_j'$. $G_2'$ is a quadratic form in $\boldsymbol{a}'$ with $N$ real eigenvalues. There are $N$ free Lagrange multipliers to potentially shift all $N$ eigenvalues to the positive side and fulfill (49). However, one can easily construct open parameter sets of $c_{ijk}$, $i, j, k = 1, \ldots, N$ for which positive definiteness of $G_2'$ cannot be obtained for arbitrary choices of $\boldsymbol{\lambda}$. Consider, for instance, $N = 2$, $c_{111} = c_{222} = 0$ from (6), $c_{122} = -c_{211} = \epsilon$, $c_{112} = c_{121} = -c_{212} = -c_{221} = 1$. As $\epsilon \to 0$, the discriminant criterion for positive definiteness requires $\lambda_1 \to \lambda_2$ which violates the necessity of $\lambda_1\lambda_2 < 0$ for positive coefficients of $\left(a_i'\right)^2$, $i = 1, 2$. Hence, (49) cannot be generically satisfied for arbitrary quadratic Galerkin system coefficients.

Similarly, also the total power balance ($K = 1$ constraint) does not generically lead to the existence of $\boldsymbol{\lambda}$ satisfying (49). The same behaviour holds for the modal power balances ($K = N$ constraints).

This is not surprising since the balance equations do not generally exhibit a robust amplitude-limiting mechanism which prevents the divergence of the Galerkin solution and which effectively limits the PDF support in the MaxEnt principle. The closure-problem re-occurs in another form in the MaxEnt framework.

#### 3.6.3. Closure strategy 1: initial manifolds

Most low-order Galerkin models are stabilized by effective inertial manifolds. Here, the amplitudes of the slowly varying base flow modes are slaved to the fluctuation levels of the oscillatory modes. Sometimes, POD decompositions contain A-modes describing slow variations of the base flow. In general, such modes need to be added to the Galerkin model [9]. Let $i = 1, \ldots, M$ be the indices of oscillatory B-modes and $i = M+1, \ldots, N$ the indices of A-modes (assuming $M < N$). Let us further assume that the A-modes span an inertial manifold in which the dynamics of the Galerkin system are embedded. Then, the slaving argument yields

$$0 = c_i + \sum_{j=1}^{N} c_{ij}\, a_j + \sum_{j=1}^{N} c_{ijk}\, a_j\, a_k, \quad i = M+1, \ldots, N.$$

Let us further assume that these equations can be solved for $a_i$, $i = M+1, \ldots, N$,

$$a_i = c_i^m + \sum_{j=1}^{M} c_{ij}^m\, a_j + \sum_{j,k=1}^{M} c_{ijk}^m\, a_j\, a_k, \quad i = M+1, \ldots, N. \tag{50}$$

Here, the superscript $m$ is a reminder that the coefficients parameterize the manifold and do not coincide with the corresponding Galerkin system coefficients. These equations may derived from the Galerkin system [21,44] or directly from the Reynolds equation [28,42,22].

The resulting Eqs. (4) for $i = 1, \ldots, M$ and (50) for $i = M+1, \ldots, N$ define a set of differential–algebraic equations (DAE), also called descriptor system. The DAE can be made a pure system of ordinary equations by substituting (50) in (4) at the expense of introducing a new cubic term:

$$\frac{da_i}{dt} = c_i^m + \sum_{i,j=1}^{M} c_{ij}^m\, a_j + \sum_{i,j,k=1}^{M} c_{ijk}^m\, a_j\, a_k + \sum_{i,j,k,l=1}^{M} c_{ijkl}^m\, a_j\, a_k\, a_l, \quad i = 1, \ldots, M. \tag{51}$$

Here, $c_i^m, \ldots, c_{ijkl}^m$ are constants derived from the original system. The corresponding total instantaneous total energy equation for $E = \sum_{i=1}^{M} a_i^2/2$ reads

$$\frac{dE}{dt} = \sum_{i=1}^{M} c_i^m\, a_i + \sum_{i,j=1}^{M} c_{ij}^m\, a_i\, a_j + \sum_{i,j,k=1}^{M} c_{ijk}^m\, a_i\, a_j\, a_k + \sum_{i,j,k,l=1}^{M} c_{ijkl}^m\, a_i\, a_j\, a_k\, a_l, \quad i = 1, \ldots, M. \tag{52}$$

No averaging is performed, this time. The fluctuation energy remains bounded if the highest-order term is stabilizing in all directions:

$$\sum_{i,j,k,l=1}^{M} c_{ijkl}^m\, a_i\, a_j\, a_k\, a_l \to -\infty \quad \text{as } \|\boldsymbol{a}\| \to \infty. \tag{53}$$

In the mean-field model, the corresponding term reads $-\beta_1^m r_1^4$.

The MaxEnt problem subject to the total power balance contains the 4th order term as its highest-order term. Hence, the stabilization condition for the Galerkin system (53) implies that (49) can be fulfilled with some Lagrangian multipliers. The construction of stable inertial manifolds satisfying (53) is a general recipe for robust Galerkin systems as well as well-posed MaxEnt closures.

*3.6.4. Closure strategy 2: assumptions for statistical moments*

One may also follow classical closure approaches. Suppose, we incorporate $N$ modal Reynolds equations (37) and $N$ modal power balances (46) as $K = 2N$ constraints (14c). This yields $N(N+1)(N+2)/3!$ independent cubic terms $a_i' a_j' a_k'$ in the exponent of (48) which make the PDF non-normalizable. Let $\zeta_i,\ i = 1, \ldots, N$ be the Lagrange multiplier conjugate to the $i$th modal power balance. Annihilation of the cubic terms can be achieved via $\zeta_1 = \zeta_2 = \cdots = \zeta_N$ due to (6). This degeneracy effectively replaces the modal power balance by its total version (44), i.e. counteracts the goal of satisfying the modal power balance.

The MaxEnt inferred PDF (48) can be made integrable by incorporating stabilizing 4th order constraints. $N$ equations of the quasi-normal approximation (47) with $i = j = k = l,\ i = 1, \ldots, N$ serve this purpose by adding (stabilizing) $\left(a_i'\right)^4$ terms which outweigh any cubic terms at infinity. The underlying hope of this technical regularization is that the quasi-Gaussian approximation is not strongly incompatible with the true solution. It may be noted that the relations of the quasi-Gaussian approximation are homogeneous, i.e. rescaling the mode amplitudes by an arbitrary factor does not change their validity. The approximation only affects the shape of the PDF.

Before engaging in this enterprise, the potential merits are estimated for the mean-field system. We apply the closure to the corresponding total power balance (23)

$$\left\langle \sigma_1 r_1^2 - \beta_1^m r_1^4 \right\rangle = 0.$$

For the periodic mean-field solution (16), the second moments are

$$\left\langle a_i a_j \right\rangle = \frac{\left\langle r_1^2 \right\rangle}{2}\delta_{ij} = \frac{R^2}{2}\delta_{ij}, \tag{54}$$

where $R$ is the radius of the limit cycle. The fourth-order term of (23) reads $\left\langle r_1^4 \right\rangle = \left\langle \left(a_1^2 + a_2^2\right)^2 \right\rangle = \left\langle a_1^4 + 2a_1^2 a_2^2 + a_2^4 \right\rangle$. Exploiting (47) and (54) yields $\left\langle r_1^4 \right\rangle = \frac{7}{2}R^4$. In contrast, the periodic solution $r_1 \equiv R$, implies $\langle r_1^4 \rangle = R^4$. The fourth moment is overpredicted by a factor 3.5! Continuing, the non-trivial solution of (23) becomes

$$\langle r_1^2 \rangle = \frac{2}{7}\frac{\sigma_1}{\beta_1^m},$$

which is about 28% of the true value. Hence, we cannot expect an accurate MaxEnt closure for the limit cycle using modal power balances and the Millionshtchikov closure as constraints. The higher-order moments of the limit-cycle solution deviate significantly from a quasi-normal distribution and (47) is a source of large errors. For Galerkin systems with broad-band dynamics, the refined MaxEnt closure can be expected to yield better predictions—bearing in mind that the Millionshtchikov closure is an ad hoc approximation.

W.K. George (private communication, 2011) experimentally observes that velocity fluctuations of turbulent shear flows satisfy the Millionshtchikov equations with high accuracy. Possibly, a Galerkin projection of these vanishing fourth-order cumulants in velocity variables provides better stabilizing fourth-order constraints than (47) in Galerkin space.

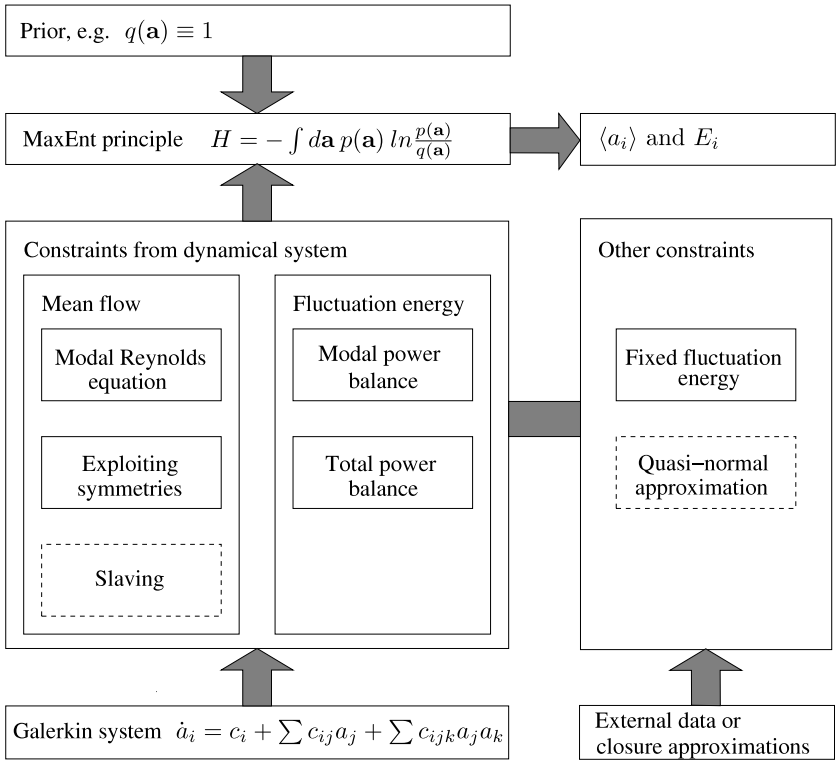


**Fig. 2.** MaxEnt closure strategy. The interface between the MaxEnt principle (top) and the Galerkin system (bottom) is the employed constraints (subset of the middle). Some constraints are derived from the Galerkin system (left), while some may be obtained from solution data or closure considerations (right). The fixed energy constraint for microcanonical ensembles foreshadows an application of Section 4. Dashed rectangles indicate approximations. The moments (top right) are obtained from the ergodic measure inferred from MaxEnt. By definition, the MaxEnt principle depends on the prior assigning an a priori PDF to the Galerkin state space.

#### *3.6.5. Closure strategy 3: empirical knowledge*

An even more imposing closure strategy is the use of solution properties. For instance, the known fluctuation energy $E$,

$$\frac{1}{2}\sum_{i=1}^{N}\left\langle \left(a_i'\right)^2 \right\rangle = E, \tag{55}$$

may be included in the constraints. This makes the PDF (48) normalizable for constraints containing only first and second moments, like the modal Reynolds equation or the total power balance.

In general the additional constraints must of same or higher order than the constraints derived from the Galerkin system. Fig. 2 comprises the strategies discussed in the latest three subsections.

## 4. Results for a wake model

In this section, the MaxEnt closure of a 7-dimensional Galerkin system is considered. The Galerkin system describes transient and post-transient oscillatory wakes from zeroth to third harmonics (Section 4.1). The MaxEnt closure strategy of the previous section is applied in Section 4.2.

### *4.1. Galerkin system for vortex shedding*

We recapitulate a Galerkin system of oscillatory laminar vortex shedding from earlier publications [21,27,11]. This system generalizes the mean-field model of Section 2 by the inclusion of second and third harmonics. In the 7-dimensional Galerkin expansion (2), $a_1$, $a_2$ are mode amplitudes of the dominant harmonics, $a_3$, $a_4$ of the second and $a_5$, $a_6$ of the third harmonics, while $a_7$ represents the shift mode (base flow deformation). The resulting Galerkin system represents 3 quadratically coupled oscillators ($a_i,\ i = 1, \ldots, 6$) and one stable mode ($a_7$) driven by the fluctuation level:

$$\frac{da_1}{dt} = (\sigma_1 - \beta\, a_7)\ a_1 - (\omega_1 + \gamma\, a_7)\ a_2 + \sum_{j,k=1}^{6} c_{1jk}\, a_j\, a_k, \tag{56a}$$

$$\frac{da_2}{dt} = (\sigma_1 - \beta\, a_7)\; a_2 + (\omega_1 + \gamma\, a_7)\; a_1 + \sum_{j,k=1}^{6} c_{2jk}\, a_j\, a_k, \tag{56b}$$

$$\frac{da_{2l-1}}{dt} = \sigma_l\, a_{2l-1} - \omega_l\, a_{2l} + \sum_{j,k=1}^{6} c_{(2l-1)jk}\, a_j\, a_k, \quad l = 2, 3, \tag{56c}$$

$$\frac{da_{2l}}{dt} = \sigma_l\, a_{2l} + \omega_l\, a_{2l-1} + \sum_{j,k=1}^{6} c_{(2l)jk}\, a_j\, a_k, \quad l = 2, 3, \tag{56d}$$

$$\frac{da_7}{dt} = \sigma_0\, a_7 + \alpha\; \left(a_1^2 + a_2^2\right). \tag{56e}$$

Here, $\sigma_1 > 0$ signifies an unstable oscillator, damped by shift mode amplitude $a_7$, while $0 > \sigma_2 > \sigma_3$ are the growth-rates of the damped oscillators driven by the quadratic term. $a_7$ quickly adjusts to the fluctuation level of the dominant oscillator with $\sigma_0 \ll -\sigma_1$ and $\alpha > 0$, On the limit cycle, the 3 oscillator frequencies are harmonically related, $\omega_l = l(\omega_1 + \gamma_7 a_7)$ for $l = 2, 3$. For details of the model and its derivation, the reader is referred to the original literature.

We emphasize that the dynamical system structure is not tied to wake flows. The same or very similar systems of coupled oscillators are obtained for POD models of 3D boundary layers [46,47], cavity flows [48], mixing layers [44], and actuated flows over aerofoils [43], just to name a few.

### 4.2. MaxEnt closure of the vortex shedding model

In this section, the Galerkin system (56) is considered as prototype of a generalized empirical Galerkin model with an inertial manifold. This system comprises the shift mode and the energy cascade from dominant to higher frequencies. It should be noted the prediction of the energy content in the three coupled oscillators due to quadratic interactions is a non-trivial task.

The starting point of the MaxEnt closure is the most accurate closure for mean-field system in Section 2.5 with a weak marginal-stability prior. This closure can easily be generalized for three harmonics.

First, the shift mode equation is slaved to the fluctuation level leading to (19). On the corresponding manifold, the 6-dimensional Galerkin system reads

$$\frac{da_1}{dt} = \left(\sigma_1 - \beta^m\, r_1^2\right)\; a_1 - \left(\omega_1 + \gamma^m\, r_1^2\right)\; a_2 + \sum_{j,k=1}^{6} c_{1jk}\, a_j\, a_k, \tag{57a}$$

$$\frac{da_2}{dt} = \left(\sigma_1 - \beta^m\, r_1^2\right)\; a_2 + \left(\omega_1 + \gamma^m\, r_1^2\right)\; a_1 + \sum_{j,k=1}^{6} c_{2jk}\, a_j\, a_k, \tag{57b}$$

$$\frac{da_{2l-1}}{dt} = \sigma_l\, a_{2l-1} - \omega_l\, a_{2l} + \sum_{j,k=1}^{6} c_{(2l-1)jk}\, a_j\, a_k, \quad l = 2, 3, \tag{57c}$$

$$\frac{da_{2l}}{dt} = \sigma_l\, a_{2l} + \omega_l\, a_{2l-1} + \sum_{j,k=1}^{6} c_{(2l)jk}\, a_j\, a_k, \quad l = 2, 3, \tag{57d}$$

where $r_1 := \sqrt{a_1^2 + a_2^2}$ like in Section 2.

The total power balance of (57) generalizes (23) by two dissipation terms $\sigma_2 \langle r_2^2 \rangle$, $r_2 := \sqrt{a_3^2 + a_4^2}$ and $\sigma_3 \langle r_3^2 \rangle$, $r_3 := \sqrt{a_5^2 + a_6^2}$ for the second and third harmonics, respectively.

Next, we maximize the Kullback–Leibler entropy with marginal stability prior

$$H = \left\langle \ln \frac{p(a_1, a_2, \ldots, a_6)}{q(a_1, a_2)} \right\rangle \stackrel{!}{=} \max \tag{58}$$

subject to normalization condition and total power balance,

$$\langle 1 \rangle = 1, \tag{59a}$$

$$\left\langle \sigma_1 r_1^2 - \beta^m r_1^4 + \sigma_2 r_2^2 + \sigma_3 r_3^2 \right\rangle = 0. \tag{59b}$$

It may be noted that $q$ as defined by (28) and used in (58) represents a proper prior in $a_1$, $a_2$ and an improper one ($q \equiv 1$) in the other directions.

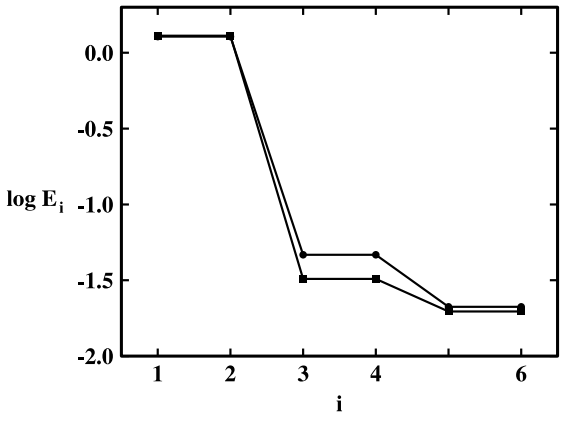


**Fig. 3.** Modal energy distributions of the Galerkin system (56) plotted on a logarithmic scale. The solid squares (■) represent the MaxEnt prediction while the solid circles (●) refer to the Galerkin solution as ground truth.

The resulting final PDF reads

$$p = \frac{q}{Z_C} \exp\left[-\zeta\left(\sigma_1 r_1^2 - \beta^m r_1^4 + \sigma_2 r_2^2 + \sigma_3 r_3^2\right)\right], \tag{60}$$

where $Z_C$ is the partition function and $\zeta$ the Lagrangian multiplier for the power balance (59b). This multiplier is determined numerically. The analytics are similar to Section 2.5. The resulting PDF for $r_1$ has a very similar shape as MaxEnt closure, shown in Fig. 1 (curve marked by '■').

The PDF (60) exactly reproduces the vanishing first and off-diagonal second moments of the employed POD modes (36). The resulting modal energy distribution

$$E_i := \left\langle a_i^2 \right\rangle / 2, \quad i = 1, \ldots, 6, \tag{61}$$

is depicted in Fig. 3 as solid squares. The values from the periodic Galerkin solution of (56) are shown as solid circles for comparison.

The energy levels are predicted with 1.2% accuracy with respect to the total fluctuation energy. It should be noted that we have formulated a complete closure. No total energy $E^\bullet$ obtained by DNS has been incorporated as constraint. The reason is that the total power constraint *on the inertial manifold* limits the effective compact support of the PDF.

### 4.3. Discussion

The total power balance (59b) plays a critical role in restricting the effective support of the PDF. In the following, bounds for energy levels of the three harmonics are derived. The total power may be decomposed in three contributions from the three oscillators, respectively:

$$P = P_{h1} + P_{h2} + P_{h3}, \tag{62a}$$

$$P_{h1} := \left\langle \sigma_1 r_1^2 - \beta^m r_1^4 \right\rangle, \qquad E_{h1} := \left\langle r_1^2 \right\rangle / 2, \tag{62b}$$

$$P_{h2} := \left\langle \sigma_2 r_2^2 \right\rangle = 2\sigma_2 E_{h2}, \quad E_{h2} := \left\langle r_2^2 \right\rangle / 2, \tag{62c}$$

$$P_{h3} := \left\langle \sigma_3 r_3^2 \right\rangle = 2\sigma_3 E_{h3}, \quad E_{h3} := \left\langle r_3^2 \right\rangle / 2. \tag{62d}$$

The subscripts $h1$, $h2$, $h3$ shall remind that the quantities represent harmonics, i.e. pairs of modes. Since $0 > \sigma_2 > \sigma_3$, the dissipative oscillators can only act as sinks, $P_{h2} \leq 0$ and $P_{h3} \leq 0$. Hence, $P = 0$ requires a source from the first oscillator $P_{h1} \geq 0$. The maximum power $P_{h1}$ can easily be estimated. The argument $\sigma_1 r_1^2 - \beta^m r_1^4$ is positive for $0 < r_1 < R$ with $R = \sqrt{\sigma_1/\beta^m}$. The argument assumes its maximum $\sigma_1 R^2/4$ at $r_{1,max} = R/\sqrt{2}$. Hence, the power $P_{h1}$ is constrained by

$$0 \leq P_{h1} \leq \sigma_1 R^2/4 =: P_{\max}. \tag{63}$$

The second harmonic energy $E_{h2}$ is bounded by the maximum energy absorption $P_{\max} + P_{h2} = 0$,

$$E_{h2} \leq -\frac{\sigma_1}{\sigma_2}\frac{R^2}{8}. \tag{64}$$

The minus sign takes into account that $\sigma_1 > 0 > \sigma_2$. Similarly, we obtain

$$E_{h3} \leq -\frac{\sigma_1}{\sigma_3}\frac{R^2}{8}. \tag{65}$$

The energy level of the dissipative oscillators is bounded by size of the limit cycle ($R$) and their decay rates $\sigma_i,\ i = 2, 3$ in relation to the growth rate $\sigma_1$.

A rigorous derivation of the energy bound of $E_{h1}$ is rather lengthy, as it involves the shape of PDF. A good estimate of the upper bound may be gained by assuming that the PDF describes exactly a limit cycle $r_1 = R_1$ in $a_1, a_2$-plane, i.e. $E_{h1} = R_1^2/2$. Then, the upper bound is derived from $P_{h1} = 0$ and yields

$$E_{h1} \leq \frac{R^2}{2}.$$

An alternative derivation of the energy bounds may be obtained by Lyapunov function-type function $V(\boldsymbol{a})$ which decays under the evolution Eq. (57) if $\|\boldsymbol{a}\|$ is sufficiently large.

## 5. Conclusions

We have generalized a maximum-entropy (MaxEnt) closure strategy for Galerkin systems of incompressible flows building on [11]. These Galerkin systems are a subclass of dissipative dynamical systems with constant-linear-quadratic propagators and an energy-preserving quadratic term. Hitherto, most MaxEnt closures have been applied to energy-preserving Hamiltonian systems with fixed energy and with coupled identical subsystems, like in the ideal gas kinetics, spin-systems, etc.

In the proposed MaxEnt framework, the turbulence closure problem re-occurs with another face: Generally, no well-conditioned MaxEnt problem can be expected if the statistical constraints are derived from the Galerkin system alone. The key enabler is distilling an amplitude-limiting mechanism—ideally without imposing any artificial or empirical relations. Most robust Galerkin models have an inertial manifold on which the trajectory is trapped in a finite domain. This manifold reduction has been used to arrive at accurate closures for the first and second moments in the two selected Galerkin systems. One alternative strategy is constraining the PDF, e.g. following Millionshtchikov closure [30] with a quasi-normal approximation. The price is a large expected inaccuracy for a limit cycle motion and assumingly smaller error for broad-band dynamics. Another alternative is imposing a known energy level from the solution as ad hoc empirical information. This might be necessary for purely POD-based Galerkin models [11]. In principle, the MaxEnt closure should become increasingly more accurate as more constraints of the Galerkin system are incorporated.

The question of the generality of the approach arises. The restriction to quadratic terms is no fundamental one, since arbitrary high-order terms can be obtained by slaving fast dynamics. The cubic term in the presented mean-field model serves as one example. Also, the energy preservation of the quadratic term only simplifies one particular closure with the total power balance. It is not necessary, if the refined modal power balance is used. In all cases, the key enabler is the identification of an amplitude-limiting constraint. Conditions for their existence have been proposed in this study.

A number of dissipative dynamical systems will require new enablers for a MaxEnt closure. For instance, the Lorenz attractor [49] has no manifold which can be exploited, but a rigorously defined attractive basin [50] which might be incorporated in the prior.

We foresee that MaxEnt closures for dynamical systems may establish a new branch of non-equilibrium statistical physics with important application to fluid mechanics. The closure is, for instance, critical for aerodynamic applications of closed-loop turbulence control [45], resolving the complex frequency cross-talk between mean force, coherent structures and actuation. The authors actively pursue these opportunities.

## Acknowledgements

We acknowledge the funding and excellent working conditions of the Chair of Excellence ‘Closed-loop control of turbulent shear flows using reduced-order models’ (TUCOROM) of the French Agence Nationale de la Recherche (ANR) and hosted by Institute PPRIME. We thank the Ambrosys Ltd. Society for Complex Systems Management and the Bernd Noack Cybernetics Foundation for additional support. R.N. was also generously supported by travel funding from the Isaac Newton Institute for Mathematical Sciences, Cambridge, UK, and a sabbatical leave from UNSW. We appreciate valuable stimulating discussions with Markus Abel, William K. George, Robert Niven, Michael Schlegel, Marc Segond, Gilead Tadmor, and Christos Vassilicos as well as the local TUCOROM team: Jean-Paul Bonnet, Laurent Cordier, Joël Delville, Peter Jordan, and Andreas Spohn. Last but not least, we thank the referees for their thoughtful and helpful suggestions.

## References

[1] J.C. Maxwell, XX—Illustrations of the dynamical theory of gases, in: W.D. Niven (Ed.), The Scientific Works of James Clark Maxwell, in: Physical Sciences, vol. 1, Cambridge University Press, Oxford, 2012, pp. 377–409.
[2] E.T. Jaynes, Information theory and statistical mechanics, Phys. Rev. 106 (1957) 620–630.
[3] E.T. Jaynes, Probability Theory. The Logic of Science, Cambridge Press, Cambridge, UK, 2003.
[4] W. Heisenberg, On the theory of statistical and isotropic turbulence, Proc. R. Soc. Lond. Ser. A 195 (1948) 402–406.
[5] L. Onsager, Statistical hydrodynamics, Nuovo Cimento (Suppl. 6) (1949) 279.
[6] T.D. Lee, Difference between turbulence in a twodimensional fluid and in a threedimensional fluid, J. Appl. Phys. 22 (1951) 524.
[7] S.F. Edwards, W.D. McComb, Statistical mechanics far from equilibrium, J. Phys. A 2 (1969) 157–171.

[8] T.M. Brown, Information theory and the spectrum of isotropic turbulence, J. Phys. A 15 (1982) 2285–2306.
[9] B.R. Noack, M. Morzyński, G. Tadmor (Eds.), Reduced-Order Modelling for Flow Control, in: CISM Courses and Lectures, vol. 528, Springer-Verlag, Vienna, 2011.
[10] P. Holmes, J.L. Lumley, G. Berkooz, C.W. Rowley, Turbulence, Coherent Structures, Dynamical Systems and Symmetry, second paperback ed., Cambridge University Press, Cambridge, 2012.
[11] B.R. Noack, R.K. Niven, Maximum-entropy closure for a Galerkin system of incompressible shear flow, J. Fluid Mech. 700 (2012) 187–213.
[12] O.A. Ladyzhenskaya, The Mathematical Theory of Viscous Incompressible Flow, Gordon and Breach, New York, London, 1963.
[13] C.A.J. Fletcher, Computational Galerkin Methods, Springer, New York, 1984.
[14] H.G. Schuster, Deterministic Chaos, second ed., VCH Verlagsgesellschaft mbH, Weinheim, 1988.
[15] A.S. Monin, A.M. Yaglom, Statistical Fluid Mechanics I, The MIT Press, Cambridge, Massachusetts, London, 1971.
[16] A.S. Monin, A.M. Yaglom, Statistical Fluid Mechanics II, The MIT Press, Cambridge, Massachusetts, London, 1975.
[17] S. Kullback, R.A. Leibler, On information and sufficiency, Ann. Math. Stat. 22 (1951) 79–86.
[18] J.N. Kapur, H.K. Kevasan, Entropy Optimization Principles with Applications, Academic Press, Boston, 1992.
[19] E.T. Jaynes, Where do we stand on maximum entropy? in: R.D. Levine, M. Tribus (Eds.), The Maximum Entropy Formalism, MIT Press, Cambridge, MA, USA, 1979, pp. 1–104.
[20] J.T. Stuart, Nonlinear stability theory, Annu. Rev. Fluid Mech. 3 (1971) 347–370.
[21] B.R. Noack, K. Afanasiev, M. Morzyński, G. Tadmor, F. Thiele, A hierarchy of low-dimensional models for the transient and post-transient cylinder wake, J. Fluid Mech. 497 (2003) 335–363.
[22] G. Tadmor, O. Lehmann, B.R. Noack, M. Morzyński, Mean field representation of the natural and actuated cylinder wake, Phys. Fluids 22 (2010) 034102-1–034102-22.
[23] G. Tadmor, B.R. Noack, Dynamic estimation for reduced Galerkin models of fluid flows, in: The 2004 American Control Conference, Paper WeM18.1, 2004, pp. 0001–0006.
[24] A. Caticha, Entropic inference and the foundations of physics, in: Brazilian Chapter of the International Society for Bayesian AnalysisISBrA, Sao Paulo, Brazil, 2012.
[25] W.V.R. Malkus, Outline of a theory of turbulent shear flow, J. Fluid Mech. 1 (1956) 521–539.
[26] D. Barkley, Linear analysis of the cylinder wake mean flow, Europhys. Lett. 75 (2006) 750–756.
[27] B.R. Noack, M. Schlegel, M. Morzyński, G. Tadmor, System reduction strategy for Galerkin models of fluid flows, Internat. J. Numer. Methods Fluids 63 (2010) 231–248.
[28] N. Aubry, P. Holmes, J.L. Lumley, E. Stone, The dynamics of coherent structures in the wall region of a turbulent boundary layer, J. Fluid Mech. 192 (1988) 115–173.
[29] E. Hopf, Statistical hydromechanics and functional analysis, J. Ration. Mech. Anal. 1 (1951) 87–123.
[30] M. Millionshtchikov, On the theory of homogeneous isotropic turbulence, C.R. Acad. Sci. U.S.S.R 32 (1941) 615.
[31] G. Schewe, Sensitivity of transition phenomena to small perturbations in flow round a circular cylinder, J. Fluid Mech. 172 (1986) 33–46.
[32] L. Boltzmann, Über die Beziehung zwischen dem zweiten Hauptsatze der mechanischen Wärmetheorie und der Wahrscheinlichkeitsrechnung, respektive den Sätzen über das Wärmegleichgewicht, in: Sitzungsbericht der Kaiserlichen Akademie der Wissenschaften, mathematisch-naturwissenschaftliche Classe, in: Abt. II, vol. LXXVI, 1877, pp. 373–435. English transl.: J. Le Roux, 2002. http://www.essi.fr/~leroux/.
[33] M. Planck, Über das Gesetz der Energieverteilung im Normalspektrum, Ann. Phys. 4 (1901) 553–563.
[34] R.S. Ellis, Entropy, Large Deviations and Statistical Mechanics, Springer-Verlag, Berlin, 1985.
[35] H. Touchette, Phys. Rep. 478 (2009) 1–69.
[36] A.N. Gorban, A.E. Gorban, G. Judge, Entropy: the Markov ordering approach, Entropy 12 (2010) 1145–1193.
[37] F. Reif, Fundamentals of Statistical and Thermal Physics, second ed., Wavelend Press Inc., Long Grove, IL, USA, 2008.
[38] R.C. Roderick, A. Maritan, A theoretical basis of maximum entropy production, in R.C. Dewar, C. Lineweaver, R. K. Niven, K. Regenauer-Lieb, (Eds.), Beyond the Second Law: Entropy Production and Non-Equilibrium Systems, Springer-Verlag, 2013 (in press).
[39] J. Guckenheimer, P. Holmes, Nonlinear Oscillations, Dynamical Systems, and Bifurcation of Vector Fields, Springer, New York, 1986.
[40] H. Haken, Synergetics, An Introduction. Nonequilibrium Phase Transitions and Self-Organizations in Physics, Chemistry, and Biology, third ed., Springer, New York, 1983.
[41] A.N. Gorban, I.V. Karlin, Invariant Manifolds for Physical and Chemical Kinetics, in: Lecture Notes in Physics, vol. 660, Springer-Verlag, Berlin, 2005.
[42] B. Podvin, A proper-orthogonal-decomposition based model for the wall layer of a turbulent channel flow, Phys. Fluids 21 (2009) 015111-1–015111-18.
[43] D.M. Luchtenburg, B. Günter, B.R. Noack, R. King, G. Tadmor, A generalized mean-field model of the natural and actuated flows around a high-lift configuration, J. Fluid Mech. 623 (2009) 283–316.
[44] B.R. Noack, P. Papas, P.A. Monkewitz, The need for a pressure-term representation in empirical Galerkin models of incompressible shear flows, J. Fluid Mech. 523 (2005) 339–365.
[45] B.R. Noack, M. Schlegel, B. Ahlborn, G. Mutschke, M. Morzyński, P. Comte, G. Tadmor, A finite-time thermodynamics of unsteady fluid flows, J. Non-Equilib. Thermodyn. 33 (2008) 103–148.
[46] D. Rempfer, F.H. Fasel, Dynamics of three-dimensional coherent structures in a flat-plate boundary-layer, J. Fluid Mech. 275 (1994) 257–283.
[47] D. Rempfer, On the structure of dynamical systems describing the evolution of coherent structures in a convective boundary layer, Phys. Fluids 6 (3) (1994) 1402–1404.
[48] C.W. Rowley, T. Colonius, R.M. Murray, Model reduction for compressible flows using POD and Galerkin projection, Physica D 189 (2004) 115–129.
[49] E.N. Lorenz, Deterministic nonperiodic flow, J. Atmospheric Sci. 20 (1963) 130–141.
[50] C. Sparrow, The Lorenz Equations: Bifurcations, Chaos, and Strange Attractors, in: Applied Mathematical Sciences, vol. 41, Springer-Verlag, New York, 1982.